Winter Precipitation Microphysics Characterized by Polarimetric Radar and Video Disdrometer Observations in Central Oklahoma

Guifu Zhang[1,2], Sean Luchs[1,2], Alexander Ryzhkov[3], Ming Xue[1,4],
Lily Ryzhkova[5], Qing Cao[2,6]

1:School of Meteorology, University of Oklahoma, Norman, Oklahoma
2: Atmospheric Radar Research Center, University of Oklahoma, Norman, Oklahoma
3: Cooperative Institute for Mesoscale Meteorological Studies, Norman, Oklahoma
4: Center for Analysis and Prediction of Storms, University of Oklahoma, Norman, Oklahoma,
5: Northwestern University, Evanston, Illinois
6: School of Electrical and Computer Engineering, University of Oklahoma, Norman, Oklahoma

Submitted to JAMC in July 2009
2nd Revision in November 2010

Corresponding author address:
Guifu Zhang
School of Meteorology, University of Oklahoma
120 David L. Boren Blvd., Suite 5900
Norman, OK 73072
E-mail: guzhang1@ou.edu

ABSTRACT

Study of precipitation in different phases is important to understanding the physical processes that occur in storms, as well as to improving their representation in numerical weather prediction models. A 2D Video Disdrometer (2DVD) was deployed about 30km from a polarimetric weather radar in Norman, Oklahoma (KOUN) to observe winter precipitation events during the 2006-2007 winter season. These events contained periods of rain, snow, and mixed-phase precipitation. Five-minute particle size distributions were generated from the disdrometer data and fitted to a gamma distribution; polarimetric radar variables were also calculated for comparison to KOUN data. It is found that snow density adjustment improves the comparison substantially, indicating the importance of accounting for the density variability in representing model microphysics.

1. Introduction

Winter precipitation can have serious consequences, but the effects seen are dependent on the type of precipitation that reaches the surface. Winter storms such as freezing rain and heavy snow are responsible for billions of dollars of damage, and can cause significant injury and death (Martner et al. 1992, Stewart 1992, Cortinas 2000, Cortinas et al. 2004). The processes that determine precipitation type can be very complex, resulting in liquid, frozen, and partially frozen precipitation (Zerr 1997). Even "warm rain" processes may result in freezing rain, increasing the complexity of winter precipitation scenarios (Rauber et al. 1994, Rauber et al 2000). An event can have freezing rain or ice pellets exclusively, periods of each, or the two may coexist (Stewart 1992); Rauber et al (2001) presented a climatology for such events in the United States. It is important to understand the microphysics of winter storms with different types of precipitation.

In general, warm rain events are studied more thoroughly than winter events (Vivekanandan et al. 1999, Zhang et al. 2006, Henson et al. 2007). While most studies using polarimetric radars focus on rain events, some analyze winter events. Ibrahim et al (1998) is one such work. Brandes et al (2007) studied the microphysics of snow in Colorado using a 2D video disdrometer. Petersen et al (2007) used a whole suite of ground, air, and space-based instruments to observe a snow event. Rasmussen et al (2003), Tokay et al (2007) and Bringi et al (2008) looked into how variations in density affect the reflectivity factor of dry snow; this issue will be explored herein for other frozen and partially frozen particles in addition to dry snow. Although most winter precipitation studies focus on dry snow, Martner et al (1993) included some mixed phase precipitation, but do not use polarimetric radar observations. Thurai et al

(2007) used polarimetric radar observations for winter precipitation not having the mixed phase.

There are also some studies that focus on various winter precipitation types. Trapp et al (2001) used a polarimetric radar to observe a winter storm event with snow and mixed-phase precipitation in Oklahoma. Barthazy et al. (2001) used polarimetric radar data for detection and classification of hydrometeor types and then verified the data with ground-based in-situ measurements. Yuter et al (2006) used a disdrometer to investigate physical properties of rain, mixed-phase, and wet snow with a disdrometer. Raga et al (1991) also focused on a winter storm with multiple types of precipitation using an instrumented plane to gather data. Instrumented aircraft is a valuable source of information – however, this method of gathering data is expensive and impractical to perform frequently over a long period of time, and in weather potentially hazardous to safety of flight (Politovich et al. 1996; Vivekanandan et al. 2001). In contrast, data collected with radar and disdrometers eliminate these short comings, and those can obtain vast amounts of data on different precipitation types. For example, during the winter of 2006-2007 data from both the National Severe Storms Laboratory's (NSSL) polarimetric KOUN radar and the University of Oklahoma 2D video disdrometer (OU 2DVD) and contains contributions from all-liquid, all-frozen, and mixed phase precipitation. The dataset allows for a quantitative comparison study to characterize the precipitation physics.

This paper will present the observations of winter precipitation in Central Oklahoma and the precipitation microphysics revealed. In section 2, the dataset collected by NSSL KOUN and OU 2DVD is described. Methods used to calculate the polarimetric variables from the disdrometer data are presented in section 3. In section 4, polarimetric radar variables calculated from the disdrometer data are then compared to radar measurements to reveal the

importance of the density variability for the observed winter events. A summary discussion and conclusions are provided in the last section.

2. Dataset

Data used for this study were collected using a S-band (11-cm wavelength) polarimetric weather radar (KOUN) and a 2D video disdrometer (2DVD). KOUN, located in Norman, Oklahoam, is a prototype WSR-88D dual-polarization radar maintained and operated by NSSL. The radar measures reflectivity factor in horizontal polarization (Z_H or Z), differential reflectivity (Z_{DR}), copolar cross correlation coefficient (ρ_{hv}), and differential phase (ϕ_{DP}) (Doviak and Zrnić, 1993), and its data has been used extensively in hydrometeor classification and rain estimation (Zrnić and Ryzhkov 1999, Straka et al. 2000, Ryzhkov et al. 2005). The two measurements most important to this study are Z_H and Z_{DR}; these values for dry snow are usually lower than those for rain (Ryzhkov and Zrnić 1998).

The OU 2DVD was deployed on the University of Oklahoma's Kessler Farm Field Laboratory (KFFL). As seen in Figure 1, KFFL is approximately 30 km from KOUN. At this distance, the disdrometer lies beyond the region of ground clutter, but, with a beam width of about 500 meters, is still close enough to the radar to ensure good resolution. In addition, the Washington site of the Oklahoma Mesonet is also located at KFFL, providing surface observations of wind and temperature. As shown in Fig.1, the OU 2DVD is a low-profile version (Schönhuber et al. 2008) — an updated version of that described by Kruger and Krajewski (2002). An example of its measurements, in the form of two images for each particle, is seen in Fig. 2.

The KOUN radar and the 2DVD data were collected during several precipitation events during the 2006-2007 winter. These events had rain, snow, and mixed phase precipitation, but most had periods of multiple types. The radar data were averages of 3x3-grid resolution volumes measured at 0.5 degrees above horizontal (i.e., 260 m above the KFFL ground). The OU 2DVD data were available for all events, resulting in 7752 one-minute particle size distributions (PSDs). To increase the number of particle samples for a more stable distribution, particularly during periods of snow, these were condensed into five-minute PSDs, the same as that of Brandes et al. (2007).

There were four events over six days for which both radar and disdrometer data were collected: 30 November 2006; 12-14 January 2007; 27 January 2007; and 15 February 2007. The first three events contained transitions from liquid precipitation to frozen precipitation, while only snow fell during the 15 February event. The days most closely examined in this paper are 30 November 2006 and 27 January 2007. The precipitation associated with the 30 November event began with convection along a cold front, and continued with stratiform precipitation. The early precipitation was primarily rain, which eventually transitioned into mixed phase precipitation, which gave way to a period of snow (Scharfenberg et al 2007). Typical particles measured by the 2DVD demonstrate this transition from raindrop (Fig. 2a) to ice pellet (Fig. 2b) and snowflakes (Fig. 2c&d). Figure 3 shows two RAOB soundings and a RUC analysis sounding for Norman, Oklahoma that corresponds to the periods of different precipitation. The 30 November 0000 UTC soundings, during a time of freezing rain, show subfreezing temperatures at the surface under a strong inversion and warm layer. A considerably shallower warm nose exists at 1200 UTC, and corresponds to a transitional period of mixed-phase precipitation. Finally, the 0000 UTC RUC analysis for 1 December shows a

column completely below freezing, and corresponds to the period of snow later in the event. The precipitation on 27 January was also associated with the passage of a cold front. The initial precipitation fell as rain. Afterwards, there was a break in precipitation, and then a second swath of precipitation fell as snow. The period of snow is interesting in that the surface temperature was still above freezing and saturation was reached, but this warm layer at the surface was not sufficiently warm or deep enough to melt the snow completely. Mesonet data shows that the surface temperature at the Washington station is lower than earlier – very near freezing, showing little opportunity for melting. See more analysis over precipitation periods in section 4.

3. Methodology

a) Calculation of Radar Variables

Using the data collected by the disdrometer, it is possible to model polarimetric radar variables for comparison with radar data. For horizontally and vertically polarized waves, the radar reflectivity factor can be calculated as (Zhang et al. 2001)

$$Z_{h,v} = \frac{4\lambda^4}{\pi^4 \left|K_w\right|^2} \int \left| f_{h,v}(D) \right|^2 N(D) dD , \qquad (1)$$

where λ is the radar wavelength, $K_w = \frac{\varepsilon_w - 1}{\varepsilon_w + 2}$, ε_w is the relative dielectric constant of water, $f_{h,v}$, are the backscattering amplitudes of hydrometeors for horizontally and vertically polarized waves, respectively, and $N(D)$ is the particle size distribution (PSD). For rain, the scattering amplitudes are found using the T-matrix scattering method. For snow, assuming that the

particles are oblate spheroids within a Rayleigh regime, the scattering amplitudes can be determined using the following equation (Ishimaru 1991):

$$f_{h,v} = \frac{\pi^2 D^3}{6\lambda^2} \frac{\varepsilon - 1}{1 + L_{h,v}(\varepsilon - 1)} . \quad (2)$$

Here, D is the equivolume sphere diameter, $L_{h,v}$ is a shape parameter, and ε is the relative dielectric constant of the particle. Further, $L_{h,v}$ are defined as:

$$L_v = \frac{1 + c^2}{c^2}\left(1 - \frac{\arctan c}{c}\right), \quad \text{where} \quad c = \sqrt{\left(\frac{a}{b}\right)^2 - 1}, \quad (3)$$

and

$$L_h = \frac{1 - L_v}{2} \quad (4)$$

where a is the semi-major axis of the particle and b the semi-minor axis. The axis ratio b/a is fixed at 0.7 for frozen particles. The PSD measured by the disdrometer is also separated into PSDs that are treated as rain and as snow, in a manner similar to Yuter et al (2006). The dielectric constant of the hydrometeor, ε, depends on the particle's composition. If it is water, $\varepsilon = \varepsilon_w$ the dielectric constant of water. If the particle is dry snow, the following Maxwell-Garnett mixing formula is used (Ishimaru, 1991):

$$\varepsilon = \varepsilon_s = \frac{1 + 2 f_v y}{1 - f_v y} . \quad (5)$$

Here, ε_s is the dielectric constant of dry snow, f_v is a fractional volume, ρ_s/ρ_i (ρ_s the density of snow and ρ_i the density of solid ice). Also, $y = (\varepsilon_i\text{-}1)/(\varepsilon_i + 2)$, where ε_i is the dielectric constant of ice. The dielectric constant are calculated at 0^oC for the 11-cm wavelength, yielding ε_w

=(80.7, 23.9) and ε_i =(3.17, 0.0039). The density of snow, as proposed by Brandes et al (2007), is:

$$\rho_s = 0.178 D^{-0.922}, \qquad (6)$$

where the diameter, D, is in millimeters and ρ_s is in grams per centimeter cubed. Eq. (6) is very similar to that of $\rho_s = 0.17 D^{-1}$ found earlier by Holroyd (1971).

From these reflectivity factors expressed by (1), we can compute the 2DVD derived $Z = 10 \log_{10}(Z_h)$ in dBZ and differential reflectivity $Z_{DR} = 10 \log_{10}(Z_h / Z_v)$. This modeled data can be compared with the Z and Z_{DR} measurements from KOUN, averaged over nine resolution volumes arranged in a 3x3 grid above KFFL.

b) Density Adjustment

It is noted that equation (6) is a statistical relation derived from disdrometer and gauge measurements of Colorado winter storms. While looking at the disdrometer data collected in Oklahoma, it became apparent that the density relation in equation (6) may not best describe the density of the snowfall during these events. Several factors could affect the density of frozen precipitation that cannot be described by one simple size-density relation. There are both in-cloud processes that affect the formation and growth of snowflakes, as well as sub-cloud processes that affect the flake during its descent to the ground (Roebber et al 2003). Figure 4 shows a plot of measured fall velocities on 30 November 2006. Also plotted is the empirically derived fall speed of rain drops (Brandes et al. 2002), and the lower curve is the empirically derived terminal velocity for snow particles (Brandes et al. 2007).

The curve plotted in the middle is used to separate the liquid and ice-phases. Of primary interest are the plotted asterisks which signify particles in the snow portion of the event, most of the snow velocities measured in Oklahoma are larger than the predicted fall velocity using the Brandes density relation determined from the Colorado data. Hence, the density of these particles should be greater than that predicted by the fixed relation (6).

Ways to improve the calculation of the dielectric constant were considered. Given that water is present in mixed-phase and wet snow particles, a Maxwell-Garnet mixture of water and snow could be used to create a more realistic dielectric constant. However, this requires knowledge of the amount of water present in a particle, which could not be directly measured by the radar or disdrometer. Thus, any mixture would have to be arbitrarily defined. In order to create a more realistic value of density, a terminal velocity-based modification to the density value was derived from the equation for terminal fall velocity (Pruppacher and Klett 1997, Eq. 10-138). The value for ρ_s from (6) is recast as a baseline density, ρ_b, the measured velocity is represented by v_m, and we use a baseline velocity v_{bs} to create an estimate of ρ_s to replace (6):

$$\rho_s = \alpha \rho_b , \tag{7a}$$

where

$$\alpha = \left(\frac{v_m}{v_{bs}} \right)^2 \frac{\rho_{aO}}{\rho_{aC}} \tag{7b}$$

Here, α is the adjustment, similar to the variable f_{rim} used in Ryzhkov et al (2008), The terminology is changed slightly for generality. While riming is frequently a significant factor in the variability of density for frozen precipitation, this adjustment is being used to estimate density variability for all factors, rather than one alone. Air densities (ρ_{aC} and ρ_{aO}) are esti-

mated from the pressures at 1742 m MSL for Marshall Station, Colorado and 344 m MSL for Washington Mesonet site on the KFFL, Oklahoma, respectively.

Since the particles in the snow PSD are treated as frozen, the density is capped at 0.92 g cm^{-3}. Figure 5 shows the adjusted densities as a function of particle size for the 30 November event. Results for these events were re-calculated using equations (6) and (7) to determine how the calculated polarimetric radar variables were affected by this density adjustment.

4. Case Studies

Using the 2DVD data, it was possible to compare reflectivity and differential reflectivity with those measured by KOUN and to study precipitation microphysics properties. Polarimetric variables were calculated from the disdrometer data using both the fixed density relationship, and the velocity-adjusted density relationship to see the impact of density variability.

a) 30 November 2006 event

Figure 6 shows the radar variables and the physical conditions for the event. As noted earlier, this event began with rain, mostly stratiform but with some convective cells, which continued through about 0800 UTC. A raindrop recorded at 0241 UTC is shown in Fig. 2a. A transitional period with mixed-phase precipitation becoming ice pellets then continued through about 1600 UTC, as confirmed by the 2DVD measurement of an ice pellet at 1302 UTC shown in Fig.2b. The rest of the day saw primarily snow, as indicated by Fig. 2c&d for two snowflakes measured at 2218 UTC. The measured rain DSDs and snow PSDs are shown in Fig. 6c. Winds measured at the Washington Mesonet site were in the vicinity of 7 m s^{-1} all the day (Fig. 6d), and surface temperature changed from about -2 ^{o}C for the rain period to below -5 ^{o}C for

the late period of snow (Fig. 6e), consistent with the phase change for the precipitating particles observed by the 2DVD.

Figure 6a and 6b show the comparison of reflectivity factor and differential reflectivity measured by KOUN and deduced from 2DVD measurements. The radar measurements are shown in solid blue, the calculations for the fixed snow density (6) are shown in red, and those for density-adjusted snow (7) are shown in green. Early in the period, through about 0400 UTC, there is a generally good comparison between Z (dBZ) and Z_{DR}(dB) measured by KOUN and calculated from 2DVD data even without the density adjustment. Just after 0400 UTC, there is a strange disconnect between the disdrometer and radar measurements. Given the otherwise good agreement between the two throughout the rain period except for this short stretch, there may have been an issue with the radar measurements. Also possible is that the rain measured by the disdrometer was part of a localized maximum in rain, and was partially or completely lost in the averaging of the KOUN resolution volumes. After this short disconnect, the comparisons for both Z and Z_{DR} are again quite good through the rest of the rain period—considering the seven orders of difference in the resolution volumes.

As the event transitions from rain to a mixed-phase event, we begin to see differences between the KOUN measurements and 2DVD calculations. Without the density adjustment, there can be significant differences – up to 15 dB for reflectivity. The underestimations by 2DVD data appeared to grow larger as the proportion of frozen precipitation increased. This is not a surprise because any portion of the PSD classified as frozen were treated as dry snow in this scheme, though they may have contained some fraction of liquid water or ice pellets, which would have larger dielectric constants and stronger radar returns than the modeled dry snow-flakes for the same size of particles. There are also differences between KOUN and the

disdrometer for Z_{DR}. When Z is underestimated by the disdrometer, so is Z_{DR}. When there is a higher concentration of frozen particles, both calculated Z and Z_{DR} are biased low.

Excluding the rain period (0000-1100 UTC), the mean Z and Z_{DR} biases are calculated as -12.04 and -0.22 dB, for the transition and snow periods (1100—2400 UTC) respectively, possibly due to the underestimation of particle density with the fixed relation (6). Using the velocity-adjusted density (7), the reflectivity and differential reflectivity are re-calculated and shown in green in Fig. 6a,b. For the snow period, the biases for Z and Z_{DR} are reduced significantly, to -4.85 and -0.062 dB respectively – less than a half of those without density adjustment. The comparisons of Z and Z_{DR} are also shown in one-one scatter plots in Fig. 7. The upper row plots are those without density adjustment and lower row ones are with density adjustment. While the correlation coefficients are not improved much, the data points align with the one-one line much better.

Throughout the entire event, many of the differences between the disdrometer calculations and the KOUN measurements have been eliminated with the density adjustment. The early rain period before 0400 UTC is quite good, save for the time of the largest differences, which have still been improved some. The disconnect seen after 0400 UTC is still present, and largely unchanged, suggesting that there was indeed an issue with the KOUN data. However, thereafter the comparisons were very good through the rest of the rain period. Both KOUN and disdrometer Z_{DR} were close during the rain period, before and after using the velocity-adjusted density

While the improvements made in the disdrometer calculations may have been modest during the rain period, it is during the mixed-phase and snow periods that they become more significant. The reflectivities for the disdrometer and KOUN are usually very close. While

there are still a few high peaks in Z_{DR} from the disdrometer, it matches with KOUN much better than using the fixed density relation. The early transition to snow is still somewhat rough – both Z and Z_{DR} calculated from the disdrometer data are rather noisy and sometimes contain more variations than in the previous scheme. However, where the previous calculations were all lower than the KOUN measurements, the new calculations tend to be closer to the KOUN measurements. As indicated by the reduction of calculated biases, the most dramatic improvement came at the end of the event for the snow period. Much of the extreme difference in the reflectivity comparison has been eliminated, though some difference continues to exist. Z_{DR} calculations and radar measurements are now very close.

The change from using the fixed density relation to one that is velocity-adjusted highlights the importance of the variability of hydrometeor density to their scattering properties. Rasmussen et al (2003), Tokay et al (2007) and Bringi et al (2008) noted a similar effect on reflectivity in dry snow data. The results from this study appear to confirm their findings and show that density variability is important in modeling not only reflectivity, but also differential reflectivity. Wet snow and mixed-phase precipitation, in addition to dry snow, experience effects from density variability. Comparisons of the volume-weighted density (Fig. 6f) with the temperature (Fig. 6d) measured at the Washington Mesonet site also provide a connection with recent work by Brandes et al (2008) and Jung and Zawadzki (2008). Both found that the terminal fall velocity of snow increased with temperature, implying a higher density.

Although the radar-disdrometer comparison is improved significantly with the density adjustment, some differences still remain. A number of sources could explain the differences. These include sampling volume difference, wind effects, and measurement errors. The KOUN resolution volume over the disdrometer is approximately 5×10^7 m^3, and is much larger than the

sampling volume of the 2DVD (about 5 m^3). The precipitation measured by KOUN and that measured by the disdrometer could be different. Although wind advection effects studied by Barthazy et al. (2001) and Rasmussen et al. (2003) could be small for this dataset because the radar beam center is only 260 m above the disdrometer for this dataset, wind effects on the 2DVD measurements could be significant by altering the air flow and causing undercatching (Nešpor et al (2000). Another issue may arise from uncertainty in the measurements. Drop mismatching and multiple drops positioned such that they appear as one particle to the disdrometer could result in errors (Thurai and Bringi 2005). Radar measurements themselves have errors: approximately 1~2 dB for Z and ~0.2 dB for Z_{DR}. Doubling these numbers would be possible for the comparison. Because of these factors, it may be unrealistic to expect a perfect match between the radar measurements and disdrometer calculations.

b) 27 January 2007 event

Figure 8 shows the results for the January 27 event. This event was unique in that it had no mixed-phase precipitation. There was one period of rain, followed by a break in precipitation, then a period of snow. In contrast to the other event, the warmest air on this day was in a shallow layer near the surface. As a result, when snow fell, it began as wet snow, and then gradually became dry snow as the warm layer cooled, and the surface temperature approached 0 ^{o}C. The Z and Z_{DR} comparisons appear to confirm this scenario. Without density adjustment, the comparison between KOUN and the disdrometer worsens as the snow begins at 1730 UTC, with the disdrometer calculations of Z and Z_{DR} lower than the corresponding KOUN measurements. As the snow becomes more like dry snow beginning at 1830 UTC, Z and Z_{DR} match more closely.

When the adjusted density relation (7) is used, the overall agreement between Z and Z_{DR} calculations and the radar measurements is good. As shown in Table 1, the mean Z and Z_{DR} biases reduce to (0.60 0.034) from (-6.37, -0.057) for that without the density adjustment. The correlations between the disdrometer results and radar measurements are shown in Fig. 9—indicating improved comparison. Although the improvement does not appear in the correlation coefficients, this may not be representative because there are only 54 data points for the statistical calculation.

Even with the improvement, there is a still a difference between the two reflectivities in the middle of the snowfall. This seems to correspond with the lowest Z_{DR} and the lowest surface temperatures. The volume-weighted density appears to approach its minimum here. Looking at the PSD shown in Fig. 8c, the particle concentration across the range of diameters seems to be lower here than at both the beginning and end of the snowfall. There are no large snowflakes, and there are definitely fewer medium-sized snowflakes. Even the number of smaller particles appears slightly lower than the surrounding PSDs. This difference also appears to correspond with a short, but noticeable increase in sustained winds and wind gusts. It is possible that these winds blew away the largest particles and were simply not recorded. There were stronger winds as the snow began, but the density of these wet particles was considerably higher, and would not be affected as much by the winds.

c) Other Events from the 2006-2007 Winter

There were two other events during the 2006-2007 winter observed by both the OU 2DVD and KOUN that are not discussed in depth in this paper. January 12-14, 2007 was another event which featured transitioning from rain in the wake of a passing cold front.

However, unlike other events, the rain shifted only to a period of mixed-phase precipitation at Kessler Farm. Scharfenberg et al (2007) noted that there was a short period of light snow near KOUN, but this was not observed at Kessler Farm. As a result, much of the distributions measured by the OU 2DVD were very similar to rain in character, and the contributions of frozen scatterers were small. Because of this, there were only modest alterations to the calculation of Z and Z_{DR}, which are already similar to that measured by KOUN.

The January 15 event, unlike the other winter precipitation events, was composed entirely of dry snow. This led to a similar situation as in the January 12-14 event. However, in this case the frozen precipitation is generally described very well by the Brandes relation, and so incorporation of the density adjustment helps little. The mean biases for (Z, Z_{DR}) are (-8.01, 0.066) without density adjustment and (-5.68, 0018) with density adjustment. Early in the period, there are small variations in density which result in some modest improvement in the calculations of polarimetric variables, particularly during the heaviest snow. Unfortunately, the snow was frequently so light during this event that concerns about the data quality from KOUN arose for later portions of the event when reflectivity was less than 0 dBZ, limiting the improvement of the comparison.

5. Conclusions and discussions

Observations of several winter precipitation events were made during 2006-2007 by the polarimetric KOUN radar and a 2D video disdrometer deployed at the Kessler Farm Field Laboratory. The disdrometer data were used to calculate radar variables of Z and Z_{DR}, which were then compared to KOUN data. Without density adjustment, the initial comparisons between the two datasets for the events showed that while the general patterns matched

throughout an event, there is not good agreement. It was also found that the scattering amplitudes of frozen precipitation could be calculated more accurately using a variable density adjustment factor, which is determined from the fall velocities measured by the disdrometer. After recalculation of the radar variables from disdrometer data, a much better agreement was found with KOUN data in most cases. The improvements were greatest when precipitation was not dominated by rain or dry snow, making it clear that variability in density has a very important role in modeling the scattering properties of winter hydrometeors of all types. The improved agreement for Z and Z_{DR} between the OU 2DVD and KOUN show that it is possible to attempt a microphysics retrieval from the KOUN data not just for rain, but for other winter hydrometeors, as well.

It is not surprising to see the variation of the comparisons as snow particle density for each storm can differ from the mean relation used for calculations. Exact agreements between the radar and disdrometer should not be expected due to differences in resolution volumes, wind effects and measurement errors as well as the change in particle density from storm to storm and time to time. However, further improvements may be made to the calculations for graupel. Following Yuter et al (2006) and creating a graupel category, as well as adjusting the density from a new baseline graupel density could result in improved density estimation for that type of precipitation. It may also help to adjust near-rain precipitation that should have their scattering amplitudes modified, but currently do not. Also, reintroducing a water-ice mixture for partially frozen precipitation could make both the rain and snow PSD categories more realistic. However, it would be necessary to find a way to deduce the amount of water present from the disdrometer data to accomplish this task. Adopting a variable function for the axis

ratio would help the axis ratio situation while keeping the relative computational efficiency of using binned disdrometer data.

Acknowledgements

This work was supported by NSF grant ATM-0608168. The authors would like to thank Drs. Edward Brandes and Richard J. Doviak for helpful discussions, Dr. Terry Schuur and others at NSSL for collecting the KOUN data, and Ms. Hyang-Suk Park for her help in working with the KOUN data. We also thank the anonymous reviewers for their comments and suggestions. The Mesonet data was collected by the Oklahoma Climate Survey (OCS). Atmospheric sounding data was provided by the University of Wyoming at http://weather.uwyo.edu/upperair/sounding.html. RUC analysis data was obtained from the NASA Langley Cloud and Radiation Research group at http://www-angler.larc.nasa.gov/cgi-bin/satimage/sounding.cgi.

References

Barthazy, E., S. Goke, J. Vivekanandan, S. M. Ellis, Detection of snow and ice crystals using polarization radar measurements: comparison between ground-based in-situ and S-Pol observation. *Atmospheric Research*, **59–60**, 137–162.

Brandes, E., G. Zhang, and J. Vivekanandan, 2002: Experiments in rainfall estimation with a polarimetric radar in a subtropical environment, *J. Atmos. Meteor*., **41**(6), 674-685.

Brandes, E.A., K. Ikeda, G. Zhang, M. Schonhuber, R.M. Rasmussen, 2007: A Statistical and Physical Description of Hydrometeor Distributions in Colorado Snowstorms Using a Video Disdrometer. *J. Appl. Meteor. Climat.*, **46**, 634-650.

Brandes, E.A., K. Ikeda, G. Thompson, 2008: Aggregate Terminal Velocity/Temperature Relations. *J. Appl. Meteor. Climat.*, **47**, 2729-2736.

Bringi, V.N., G. Huang, D. Hudak, R. Cifelli, S.A. Rutledge, 2008: A Methodology to Derive Radar Reflectivity-Liquid Equivalent Snow Rate Relations Using C-Band Radar and a 2D Video Disdrometer. *Proceedings, Fifth European Conference on Radar in Meteorology and Hydrology*, Helsinki, Finland.

Cortinas, J., 2000: A climatlogy of freezing rain in the Great Lakes region of North America. *Mon. Wea. Rev.*, **128**, 3574–3588.

Cortinas, J.V., B.C. Bernstein, C.C. Robbins, J.W. Strapp, 2004: An Analysis of Freezing Rain, Freezing Drizzle, and Ice Pellets across the United States and Canada: 1976–90. *Wea. Forecasting*, **19**, 377-390.

Doviak, R.J. and D.S. Zrnić, 1993: *Doppler Radar and Weather Observations*. 2nd Ed. Academic Press. 562 pp.

Henson, W., R. Stewart, B. Kochtubajda, 2007: On the precipitation and related features of the 1998 Ice Storm in the Montréal area. *Atmospheric Research*, **83**, 36-54.

Ibrahim, I.A., V. Chandrasekar, V.N. Bringi, P.C. Kennedy, P.C., M. Schoenhuber, H.E. Urban, W.L. Randen, 1998: Simultaneous multiparameter radar and 2D-video disdrometer observations of snow. *Geoscience and Remote Sensing Symposium Proceedings, IGARSS '98*, pp.437-439 vol.1.

Ishimaru, A., 1991: *Electromagnetic Wave Propagation, Radiation, and Scattering*. Prentice-Hall. 637 pp.

Jung, E. and I. Zawadzki, 2008: A study of variability of snow terminal fall velocity. *Proceedings, Fifth European Conference on Radar in Meteorology and Hydrology*, Helsinki, Finland.

Holroyd, E. W., III, 1971: The meso- and microscale structure of Great Lakes snowstorm bands—A synthesis of ground measurements, radar data, and satellite observations. Ph.D. dissertation, State University of New York at Albany, 148 pp.

Kruger, A. and W.F. Krajewski, 2002: Two-Dimensional Video Disdrometer: A Description. *J. Atmos. Tech.*, **19**, 602-617.

Martner, B.E., R.M. Rauber, R.M. Rasmussen, E.T. Prater, M.K. Ramamurthy, 1992: Impacts of a Destructive and Well-Observed Cross-Country Winter Storm. *Bull. Amer. Meteor. Soc.*, **73**, 169-172.

Martner, B.E., J.B. Snider, R.J. Zamora, G.P. Byrd, T.A. Niziol, and P.I. Joe, 1993: A Remote-Sensing View of a Freezing-Rain Storm. *Mon. Wea. Rev.*, **121**, 2562-2577.

Nešpor, V., W.F. Krajewski, A. Kruger, 2000: Wind-Induced Error of Raindrop Size Distribution Measurement Using a Two-Dimensional Video Disdrometer. *J. Atmos. Tech.*, **17**, 1483-1492.

Petersen, W.A. and Coauthors, 2007: NASA GPM/PMM Participation in the Canadian CLOUDSAT/CALIPSO Validation Project (C3VP): Physical Process Studies in Snow. *33rd International Conference on Radar Meteorology*, Cairns, Australia.

Politovich, M. K., 1996: Response of a research aircraft to icing and evaluation of severity indices. *J. Aircraft,* **33,** 291–297.

Pruppacher, H. R., and J. D. Klett, 1997: *Microphysics of Clouds and Precipitation*. Kluwer Acad. 954 pp.

Raga, G.B., R.E. Stewart, N.R. Donaldson, 1991: Microphysical Characteristics through the Melting Region of a Midlatitude Winter Storm. *J. Atmos. Sci.*, **48**, 843-855.

Rasmussen,R., A. J. Heymsfield, 1987: Melting and shedding of graupel and hail. Part I: Model physics. *J. Attmos. Sci.,* 44, 2754-2763.

Rasmussen,R., M. Dixon, S. Vasiloff, F. Hage, S. Knight, J. Vivekanandan, M. Xu, 2003: Snow Nowcasting Using a Real-Time Correlation of Radar Reflectivity with Snow Gauge Accumulation, *J. Appl. Meteor.,* 42(1), 20-36.

Rauber, R.M., M.K. Ramamurthy, A. Tokay, 1994: Synoptic and Mesoscale Structure of a Severe Freezing Rain Event: The St. Valentine's Day Ice Storm. *Wea. Forecasting*, **9**, 183-208.

Rauber, R.M., L.S. Olthoff, M.K. Ramamurthy, K.E. Kunkel, 2000: The Relative Importance of Warm Rain and Melting Processes in Freezing Precipitation Events. *J. Appl. Meteor.*, **39**, 1185-1195.

Rauber, R.M., L.S. Olthoff, M.K. Ramamurthy, D.Miller, K.E. Kunkel, 2001: A Synoptic Weather Pattern and Sounding-Based Climatology of Freezing Precipitation in the United States East of the Rocky Mountains. *J. Appl. Meteor.*, **40**, 1724-1747.

Roebber, P.J., S.L. Bruening, D.M. Schultz, J.V. Cortinas Jr., 2003: Improving Snowfall Forecasting by Diagnosing Snow Density. *Wea. Forecasting*, **18**, 264-287.

Ryzhkov, A.V., and D.S. Zrnić, 1998: Discrimination between rain and snow with a polarimetric radar. *J. Appl. Meteor.*, **37**, 1228–1440.

Ryzhkov, A.V., T.J. Schuur, D.W. Burgess, P.L. Heinselman, S.E. Giangrande, D.S. Zrnić, 2005: The Joint Polarization Experiment: Polarimetric Rainfall Measurements and Hydrometeor Classification. *Bull. Amer. Meteor. Soc.*, **86**, 809-824.

Ryzhkov, A.V., G. Zhang, S. Luchs, L. Ryzhkova, 2008: Polarimetric Characterisitics of Snow Measured by Radar and 2D Video Disdrometer. *Proceedings, Fifth European Conference on Radar in Meteorology and Hydrology*, Helsinki, Finland.

Scharfenberg, K., K. Elmore, C. Legett, T. Schuur, 2007: Analysis of Dual-Pol WSR-88D Base Data Collected During Three Significant Winter Storms. *Preprints, 33rd Int. Conf. on Radar Meteorology*, Cairns, Queensland, Australia, Amer. Meteor. Soc.

Schönhuber, M., G. Lammer, W.L. Randeu, 2008: The 2D-Video-Distrometer. *Precipitation: Advances in Measurement, Estimation and Prediction*. Springer. pp. 3-31.

Stewart, R. E., J. D. Maarwitz, J. C. Pace, R. E. Carbone, 1984: Characteristics through the melting layer of stratiform clouds. *J. Atmos. Sci.*, **41**, 3227-3237.

Stewart, R. E., 1992: Precipitation types in the transition region of winter storms. *Bull. Amer. Meteor. Soc.*, **73**, 287–296.

Straka, J.M., D.S. Zrnić, and A.V. Ryzhkov, 2000: Bulk Hydrometeor Classification and Quantification Using Polarimetric Radar Data: Synthesis of Relations. *J. Appl. Meteor.*, **39**, 1341-1372.

Thurai, M. and V.N. Bringi, 2005: Drop Axis Ratios from a 2D Video Disdrometer. *J. Atmos. Oceanic. Tech.*, **22**, 966-978.

——, D. Hudak, V.N. Bringi, G.W. Lee, B. Sheppard, 2007: Cold Rain Event Analysis Using 2-D Video Disdrometer, C-Band Polarimetric Radar, X-Band Vertically Pointing Doppler Radar and POSS. *Preprints, 33rd Int Conf. on Radar Meteorology*, Cairns, Queensland, Australia, Amer. Meteor. Soc.

Tokay, A., V.N. Bringi, M. Schonhuber, G.J. Huang, B. Sheppard, D. Hudak, D.B. Wolff, P.G. Bashor, W.A. Petersen, G. Skofronick-Jackson, 2007: Disdrometer Derived Z-S Relations In South Central Ontario, Canada. *Preprints, 33rd Int. Conf. on Radar Meteorology*, Cairns, Queensland, Australia, Amer. Meteor. Soc.

Trapp, R.J., D.M. Schultz, A.V. Ryzhkov, R.L. Holle, 2001: Multiscale Structure and Evolution of an Oklahoma Winter Precipitation Event. *Mon. Wea. Rev.*, **129**, 486-501.

Vivekanandan, J., S. M. Ellis, R. Oye, D. S. Zrnic, A. V. Ryzhkov, and J. Straka, 1999: Cloud microphysics retrieval using S-band dual-polarization radar measurements. *Bulletin of the American Meteorological Society*, **80,** 381-388.

Vivekanandan, J., G. Zhang, M. K. Politovich, 2001: An assessment of droplet size and liquid water content derived from dual-wavelength radar measurements to the application of aircraft icing detection. *J. Atmos. Oceanic. Technol.*, **18**(11), 1787-1798

Yuter, S.E., D.E. Kingsmill, L.B. Nance, M. Loffler-Mang, 2006: Observations of Precipitation Size and Fall Speed Characteristics within Coexisting Rain and Wet Snow. J. *Appl. Meteor.*, **45**, 1450-1464.

Zerr, R., 1997: Freezing rain: An observational and theoretical study. *J. Appl. Meteor.*, **36**, 1647-1661.

Zhang, G., J. Vivekanandan, and E. Brandes, 2001: A method for estimating rain rate and drop size distribution form polarimetric radar measurements. *IEEE Trans. on Geoscience and Remote Sensing*, **39**(4), 831-841.

Zhang, G., J. Sun, and E. A. Brandes, 2006: Improving parameterization of rain microphysics with disdrometer and radar observations. *J. Atmos. Sci.*, **63** (4): 1273-1290.

Zrnić, D.S. and A.V. Ryzhkov, 1999: Polarimetry for Weather Surveillance Radars. *Bull. Amer. Meteor. Soc.*, **80**, 389-406.

Table 1: Comparison of radar variables between disdrometer and radar measurements

Case	11/30/2006 (1100-2400 UTC)		1/27/2007 (1600-2400 UTC)		2/15/2007 (0000-8000 UTC)	
Variables↓	No density adj.	With density adj.	No density adj.	With density adj.	No density adj.	With density adj.
$\left\langle Z^{(D)} \right\rangle$, dBZ	10.47	17.26	16.53	22.30	0.14	2.47
$\left\langle Z_{DR}^{(D)} \right\rangle$, dB	0.653	0.741	0.483	0.574	0.624	0.672
$\left\langle Z^{(D)} - Z^{(R)} \right\rangle$,dB	-11.64	-4.85	-6.37	-0.60	-8.01	-5.68
$\left\langle Z_{DR}^{(D)} - Z_{DR}^{(R)} \right\rangle$,dB	-0.149	-0.062	-0.057	0.034	-0.066	0.018

Figure Captions

Figure 1. A representative PPI from KOUN showing the locations of the radar and Kessler Farm, as well as the OU 2DVD.

Figure 2. Typical images of particles from the OU 2DVD. Panel (a) is a raindrop recorded at 0241 UTC, panel (b) an ice pellet at 1302 UTC, panels (c) and (d) are snowflakes at 2218 UTC.

Figure 3. Atmospheric soundings for Norman, Oklahoma corresponding to the three precipitation types for the 30 November 2006 event from RAOBs (Oolman) measurement and RUC analysis. Panel (a) is 0000 UTC on November 30, (b) is 1200 UTC on the same day, and (c) is 0000 UTC on December 1 – no radiosonde was launched at this time.

Figure 4. Plot of fall velocity (ms^{-1}) versus diameter (mm) on November 30, 2006. Data from the freezing rain period (00-08 UTC) are denoted by a circle, the mixed phase period (08-16 UTC) as an 'x', and the frozen precipitation period (16-24 UTC) with a '*'. Also plotted are a fourth degree polynomial approximation of raindrop terminal fallspeed, a power-law relation for the terminal fallspeed of snow, and the velocity function used to separate the rain and snow PSDs.

Figure 5. Velocity-adjusted density versus diameter for November 30, 2006. Also plotted is the baseline density, from Brandes et al (2007).

Figure 6. Comparison of (a) Z and (b) Z_{DR} between KOUN measurements and 2DVD calculations with and without density adjustment for 30 November 2006 event. Also shown are (c) measured DSDs and PSDs, (d) wind speed and gusts measured at WASH, (e) surface temperature measurements at WASH, and (f) derived volume-weighted

density.

Figure 7. Scatter plots of 2DVD calculated Z and Z_{DR} with and without density adjustment versus KOUN measurements for 30 November 2006 event. (a) Z without density adjustment, (b) Z_{DR} without density adjustment, (c) Z with density adjustment, and (d) Z_{DR} with density adjustment.

Figure 8. As in Figure 6, but for January 27, 2007.

Figure 9. As in Figure 7, but for January 27, 2007.

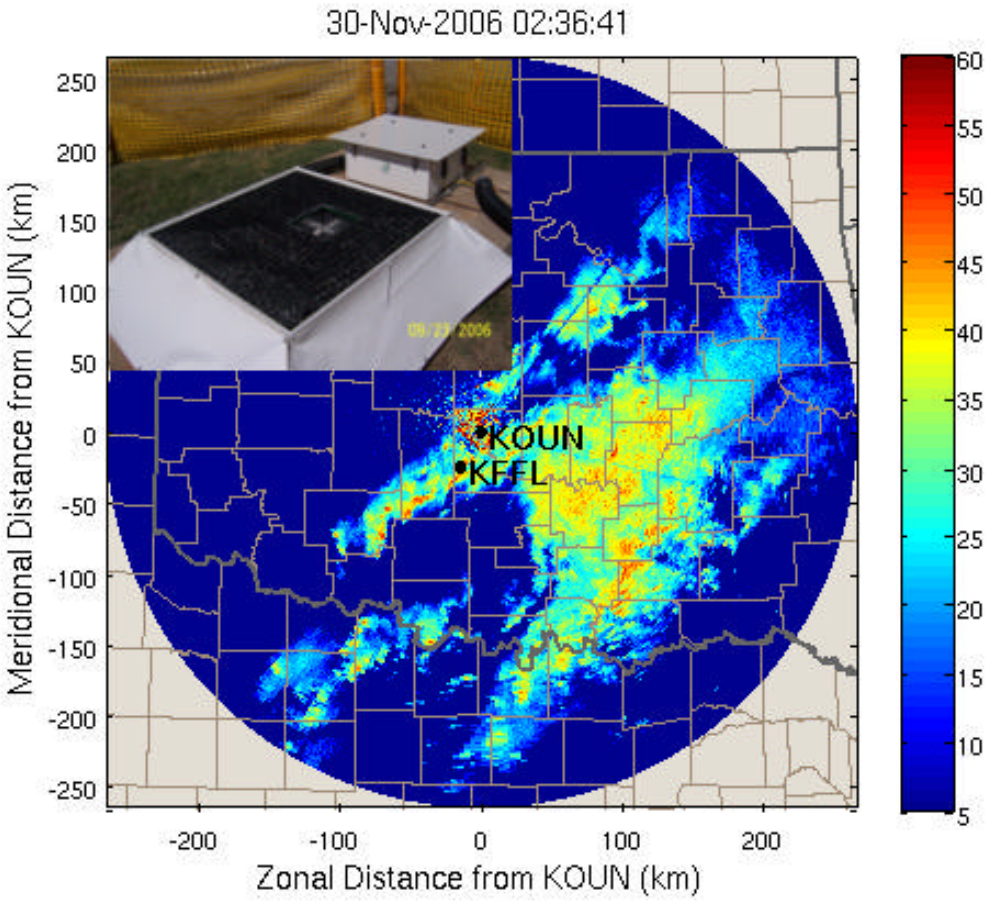

Figure 1. A representative PPI from KOUN showing the locations of the radar and Kessler Farm, as well as the OU 2DVD.

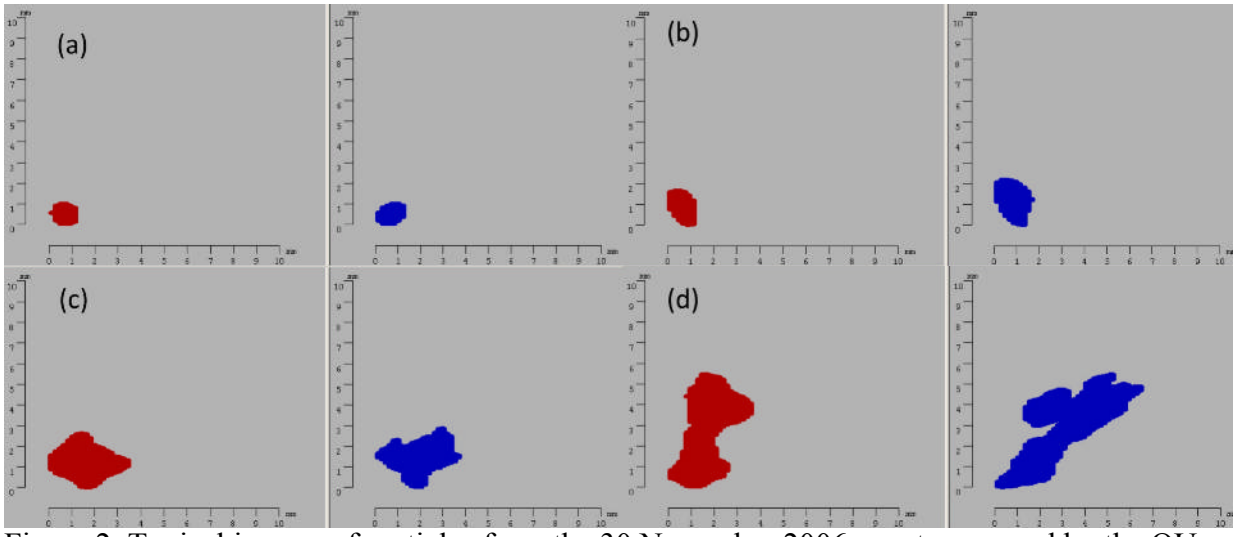

Figure 2. Typical images of particles from the 30 November 2006 event measured by the OU 2DVD. Panel (a) is a rain drop recorded at 0241 UTC, panel (b) an ice pellet at 1302 UTC, panels (c) and (d) are snowflakes at 2218 UTC.

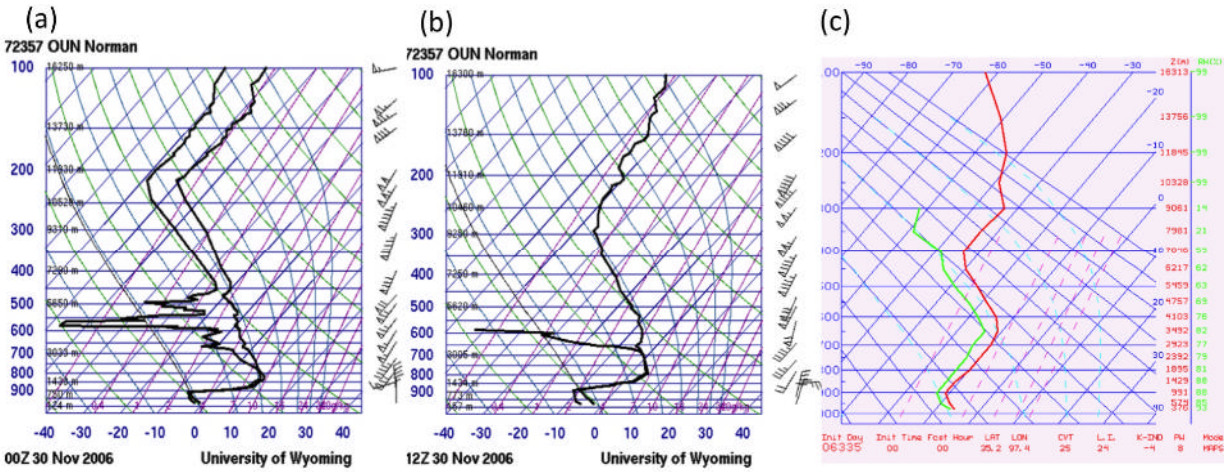

Figure 3. Atmospheric soundings for Norman, Oklahoma corresponding to the three precipitation types for the November 30, 2006 event from RAOBs (Oolman) measurements and RUC analysis. Panel a is 0000 UTC on November 30, b is 1200 UTC on the same day, and c is 0000 UTC on December 1 from RUC analysis – no radiosonde was launched at this time.

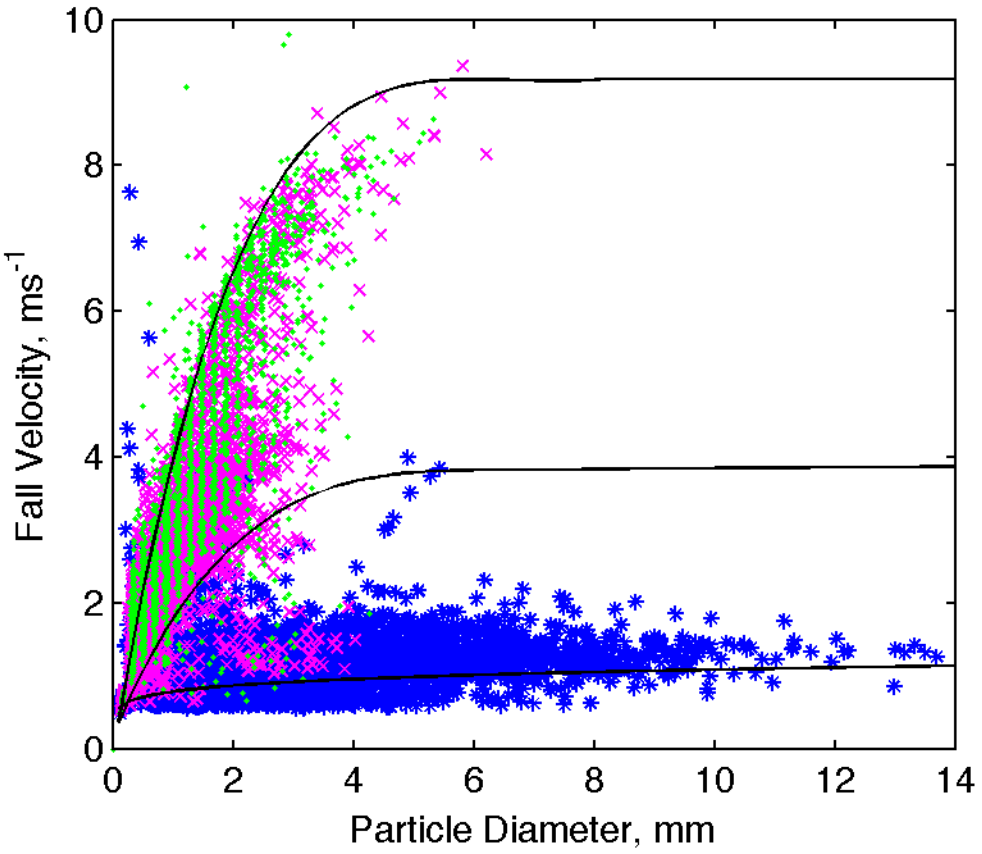

Figure 4. Plot of fall velocity (ms^{-1}) versus diameter (mm) on November 30, 2006. Data from the freezing rain period (00-08 UTC) are denoted by a circle, the mixed phase period (08-16 UTC) as an 'x', and the frozen precipitation period (16-24 UTC) with a '*'. Also plotted are a fourth degree polynomial approximation of raindrop terminal fallspeed, a power-law relation for the terminal fallspeed of snow, and the velocity function used to separate the rain

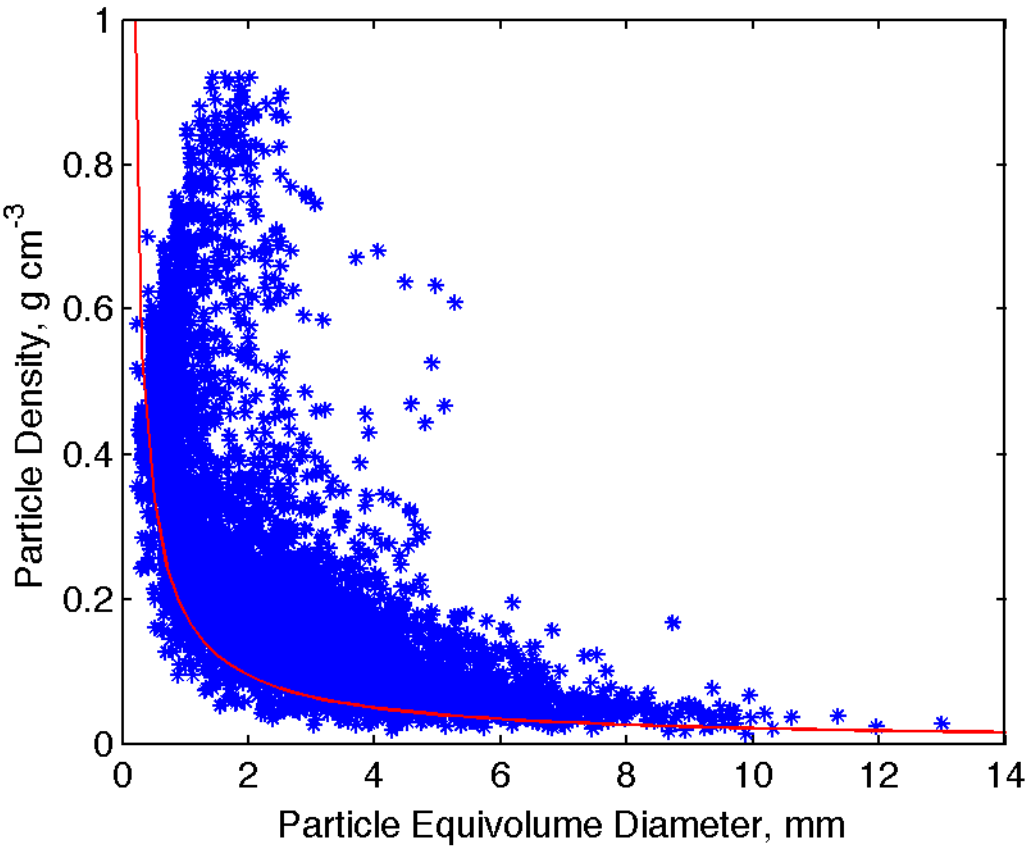

Figure 5: Velocity-adjusted density versus diameter. Also plotted is the baseline density from Brandes et al. (2007)

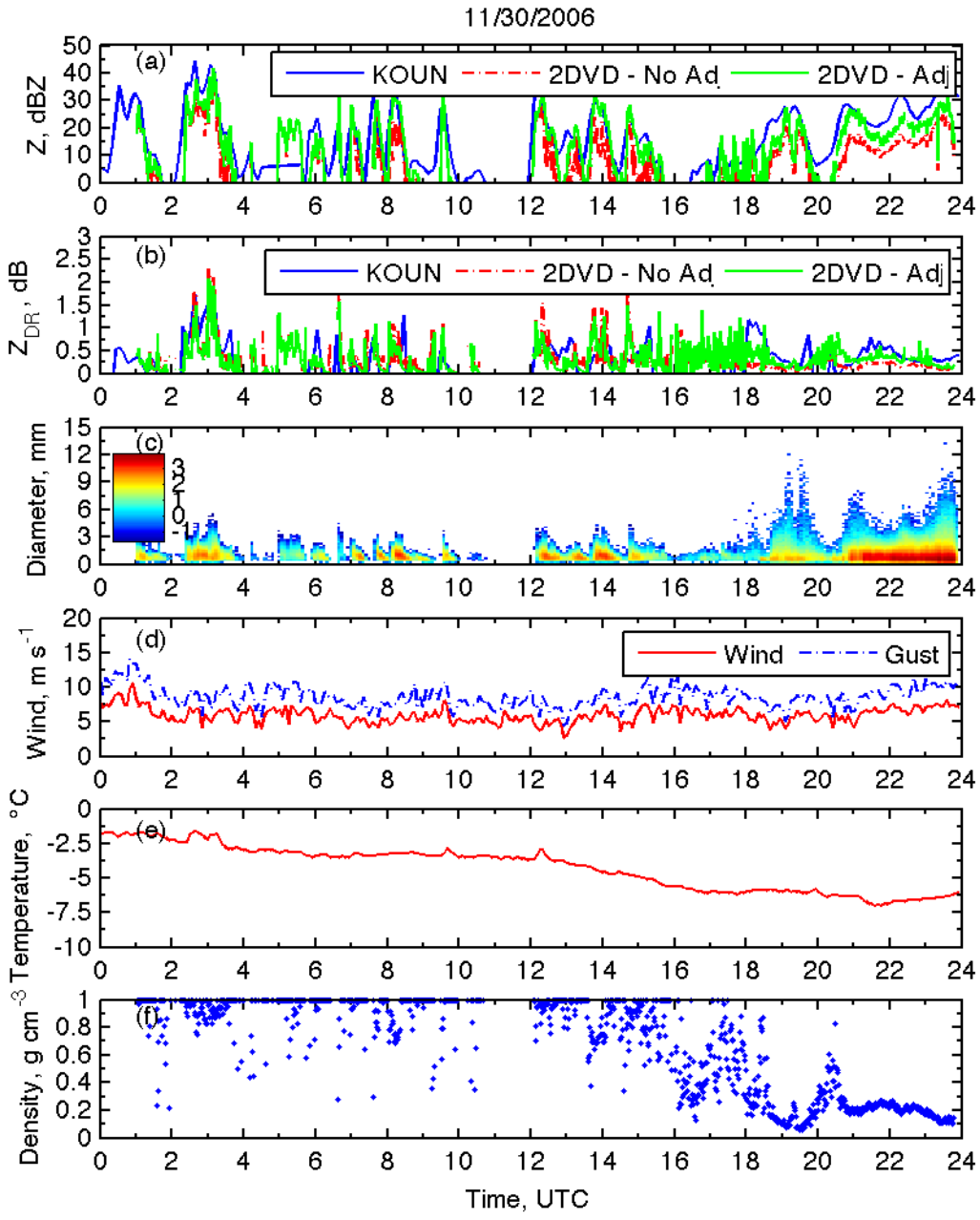

Figure 6. Comparison of (a) Z and (b) Z_{DR} between KOUN and OU 2DVD on November 30 using the velocity adjustment to the baseline Brandes density. Also shown are (c) measured DSDs and PSDs, (d) wind speed and gust, (e) surface temperature, and (f) volume-weighted density.

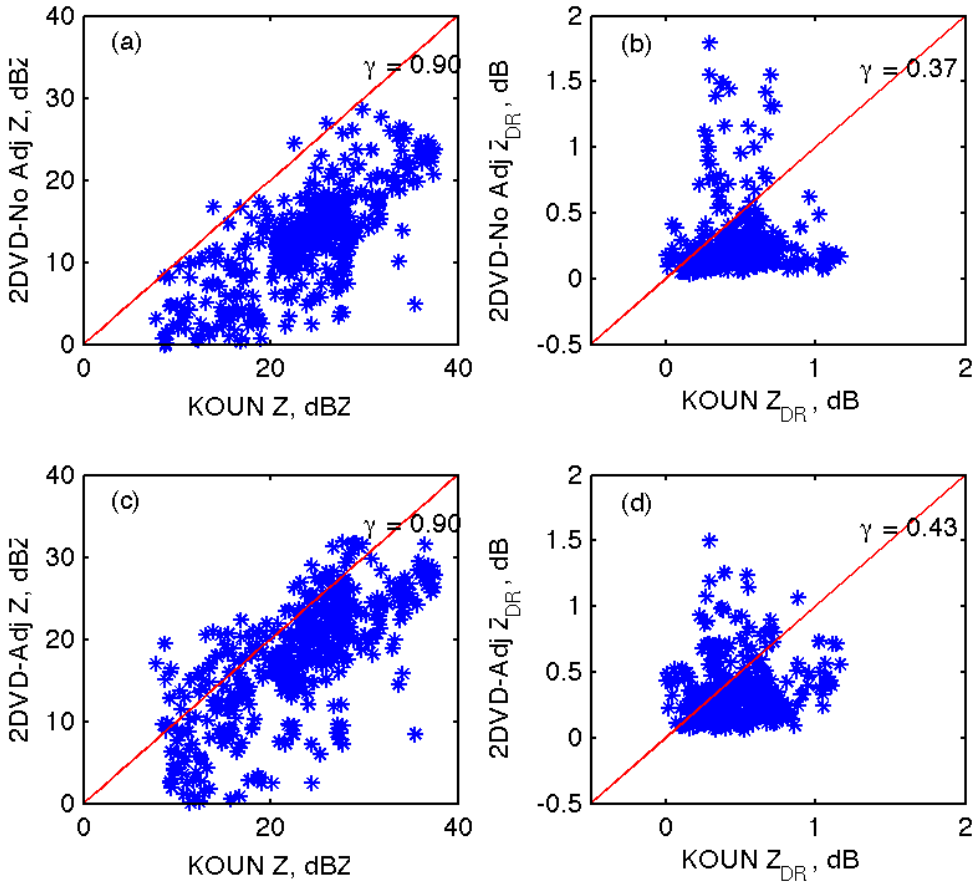

Figure 7. Scatter plots of radar-disdrometer comparisons for a) Z and b) Z_{DR} before density adjustment and c) Z and d) Z_{DR} after density adjustment.

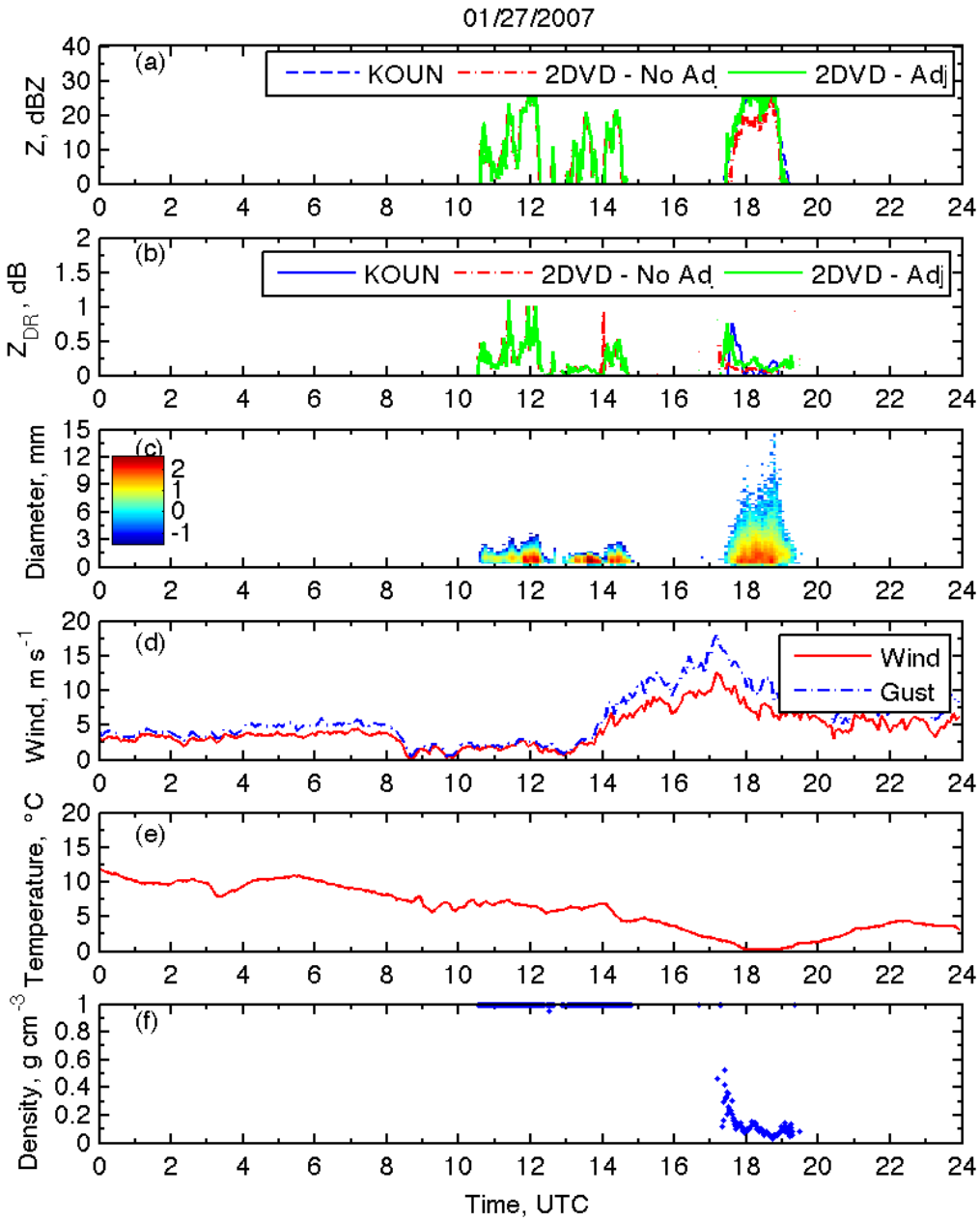

Figure 8. As in Figure 7, but for January 27, 2007.

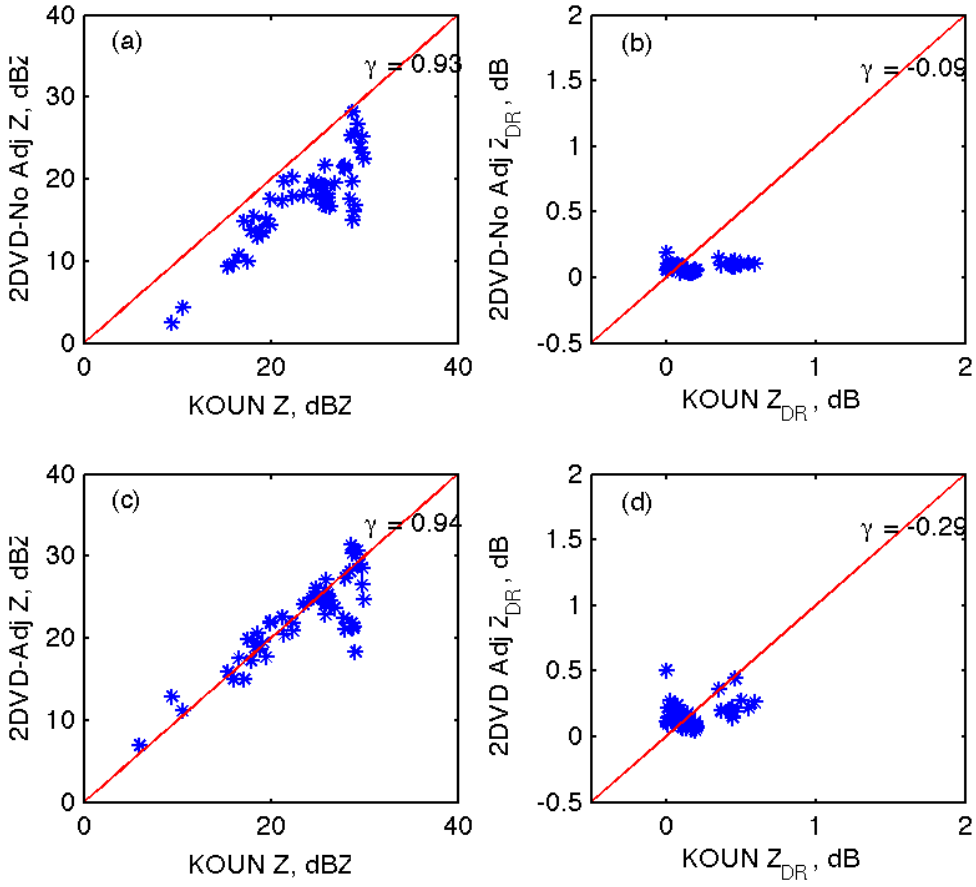

Figure 9: As in Figure 7, but for January 27, 2007.